Jonas Osburg*, Daniel Wulff*, and Floris Ernst

Generalized Automatic Probe Alignment based on 3D Ultrasound

https://doi.org/10.1515/cdbme-2022-0015

Abstract: Acquiring reproducible ultrasound images of high quality is challenging in ultrasound imaging. While physicians can rely on their experience, robot-assisted systems must be able to automatically align the ultrasound probe with the correct orientation. This paper describes a method to align the central axis of the probe to the surface normal at the point of contact. This is done by analyzing the area of ultrasound volumes directly below the transducer of the probe. A convolutional neural network is trained to estimate the inclination of the probe orientation towards the direction of the surface normal. Experiments on two different phantoms indicate that the mean absolute angle error between the estimated rotation and the ground truth surface normal are $5.0 \pm 2.8^{\circ}$. The method is able to keep the probe-surface contact continuous and the results indicate that the method is invariant to anatomical structures.

Keywords: robot guided ultrasound, convolutional neural network

1 Introduction

Robot guided ultrasound (US) enables automatic US scanning with high accuracy and reproducibility [1]. The image quality mainly depends on the contact force [2] as well as the orientation of the US probe [3]. It is concluded in [4] and [5] that an orientation along the normal of the surface leads to improved image quality. For that reason in [6] a method for an automatic robot-assisted US system was presented, which combines force estimations as well as real-time US images to determine the optimal probe orientation. The aim was to align the central axis of an US probe, which is attached to the endeffector of a robot, with the tissue surface normal. Although promising results were achieved, some limitations remain: At every position a fan motion has to be performed to orient the probe correctly in the out-of-plane direction. When an US scan consisting of many points is required, this may result in a long treatment time, reduced patient comfort and thus limit the applicability.

*Corresponding author: Jonas Osburg, Daniel Wulff, Floris Ernst, Institute for Robotics and Cognitive Systems, Ratzeburger Allee 160, Lübeck, Germany, e-mail: {osburg, wulff}@rob.uni-luebeck.de

Jonas Osburg and Daniel Wulff: contributed equally.

In this paper, we present a one step method to align the central axis of an US probe attached to a robot approximately normal to the surface of the scanned tissue on the basis of 3D US volumes. A Convolutional Neural Network (CNN) estimates the angle towards the surface normal such that the robot can correct the probe orientation immediately.

2 Methods

Following, the data acquisition and preparation as well as the execution and evaluation of the experiments is described.

2.1 Data Acquisition

The acquisition of training data is done with a KUKA LBR iiwa 7 R800 robot and a Philips Epiq 7 US station with the XL14-3 probe at different locations on two leg phantoms and one torso phantom (see Figure 1 A-C). US volumes are acquired at six different locations on the torso phantom, at four different locations on the transparent leg phantom and at two locations on the red leg phantom. First, the probe is aligned by hand at a chosen location. The probe has full contact to the phantom surface and the orientation is approximately aligned to the surface normal though no ground truth is known. To acquire data with different contact angles at the contact point, in a second step, the probe orientation is varied in a range from -15° to 15° at a step size of 3° as visualized in Figure 2. This is done by rotating the probe around the ^{tcp}y - and ^{tcp}x -axis of the tcp-frame, which is located in the center of the probe as shown in Figure 2. $\Delta\theta_{\rm IP}$ and $\Delta\theta_{\rm OP}$ represent the angles by which the probe must be rotated to be aligned with the approximate surface normal in the in-plane and out-of-plane directions, respectively (see Figure 2). First, the probe is rotated around its ^{tcp}y -axis by a corresponding angle of $\Delta\theta_{\rm IP}$ while $\Delta\theta_{\rm OP} = 0^{\circ}$. Afterwards, the probe is rotated around its ^{tcp}x axis by a corresponding angle of $\Delta\theta_{OP}$ while $\Delta\theta_{IP}=0^{\circ}$. In addition, the probe pressure force onto the phantom surface is varied for each probe orientation. The probe is moved in 2 mm steps in the ^{tcp}z -direction until a depth of 10 mm is reached. This varies the range of contact forces that occur with the aim of achieving a higher data variability. During this process, the US data as well as the force and position data provided by the robot are stored.

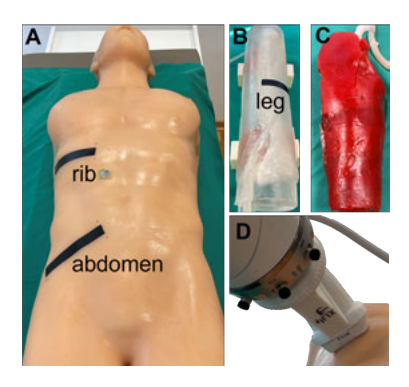


Fig. 1: Phantoms for data acquisition and validation. (A): Torso phantom. (B), (C): Leg phantoms. The validation scans are marked with black tape. (D): US probe attached to robot endeffector while doing a validation scan at the rib.

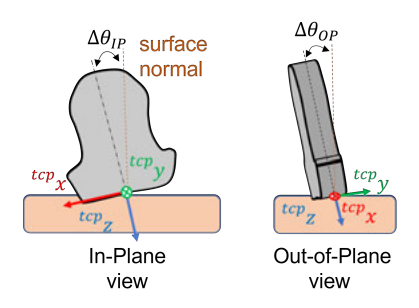


Fig. 2: For data acquisition, the probe orientation was varied between -15° and 15° in steps of 3°.

2.2 Data Preparation

After acquisition, the data is prepared for CNN training. The proposed approach for estimating the required US probe rotation angles $\Delta\theta_{\rm IP}$ and $\Delta\theta_{\rm OP}$ is based on both forces and images. Depending on the area of interest, US volumes can contain highly different anatomical structures. To get an approach that is invariant to this structural variability, we propose to not use the whole US volume but only the area directly under the US probe. This transducer area, marked in Figure 3, has no information about the anatomical structure but about the probesurface contact. Transducer area patches are cut out from the US volumes at a depth of 30 px as visualized in Figure 3. In a second step, these patches are resampled into a size of $30 \text{ px} \times 30 \text{ px} \times 30 \text{ px}$. To extend the available data set, random intensity rescaling is applied to the patches so that 12,548 data samples are available for training. The measured forces f_E are given in the end-effector coordinate system. The forces f_E are transferred into the US probe coordinate system to get the forces f_P by applying the transformation matrix ET_P which is known from the CAD model of the probe holder (see Figure 1 (D)). Using the probe pressure force f_P for angle estimation is an important aspect since the US image quality can be affected by both pressure and orientation due to the soft and flexible

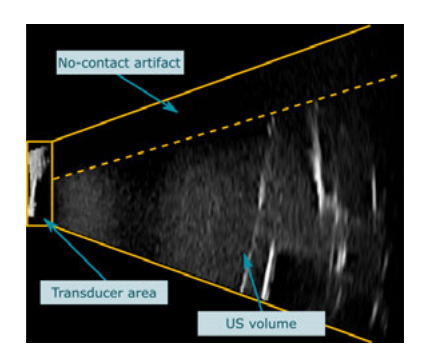


Fig. 3: A slice of a 3D US volume acquired at a probe orientation of $\Delta\theta_{\rm IP}=0^\circ$, $\Delta\theta_{\rm OP}=-12^\circ$. The transducer and the non-contact artifact are marked.

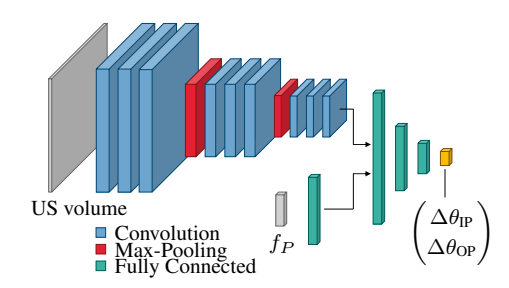


Fig. 4: Visualization of the CNN architecture. It gets an US volume and a force vector as input and predicts the required rotation angles $\Delta\theta_{\rm IP}$ and $\Delta\theta_{\rm OP}$.

skin of humans or phantoms. In addition, a rough estimation for the rotation direction D_T is calculated by determining the US volume moment M (see eq. 1).

$$M = \sum_{x,y,z} x^i y^j z^k I(x,y,z) \tag{1}$$

Here, I(x,y,z) is the US volume intensity at position (x,y,z). As can be seen in Figure 3, volumes acquired at a suboptimal probe orientation contain a shadow artifact that extends over the entire depth of the US volume. Due to that, the volume moment is shifted into the opposite direction. According to this, the parameter D_T is set to -1 or 1 depending on the shift direction of the volume moment for the in-plane and out-of-plane angles of the US probe. It should be noted that D_T could also be received by labeling the data, determining the volume moment is done to avoid the time-consuming labeling process.

2.3 Convolutional Neural Network

The required probe rotation is estimated using a twodimensional Regression CNN visualized in Figure 4. The CNN consists of nine convolutional layers with relu activation function, two max-pooling layers and four fully connected layers with sigmoid activation function. In the output layer a linear activation function is used. The CNN gets a 30 px×30 px×30 px sized volume and the force vector f_P as input. Since the CNN used is a two-dimensional model, the information along the depth axis of the US volume is handled as 30 different channels inside the CNN. Output of the model are the angle predictions $\Delta\theta_{\rm IP}$ and $\Delta\theta_{\rm OP}$ for the required rotation of the US probe. Training is performed using the rmsprop optimizer with a batch size of 128, validation split of 10 %, early stopping, exponential learning rate decay and a custom loss function, given in eq. 2.

$$Loss = L_{Rotation} + L_{Direction}$$
 (2)

Here, $L_{Rotation}$ (see eq. 3) calculates the difference between the predicted US probe rotation and the ground truth considering the rotation matrices R_P and R_T using the Frobenius norm.

$$L_{Rotation} = ||R_P - R_T||_F \tag{3}$$

The rotation matrix prediction R_P is generated using the predicted angles $\Delta\theta_{\rm IP}$ and $\Delta\theta_{\rm OP}$ while R_T is known from the data acquisition. By using $L_{Direction}$ (see eq. 4), predictions are penalized even stronger if the direction of the predicted rotation is wrong.

$$L_{Direction} = \begin{cases} 1, & \text{if } D_P \neq D_T \\ 0, & \text{otherwise} \end{cases} \tag{4}$$

Here, $D_P = \frac{\Delta \theta_{\text{IP, OP}}}{|\Delta \theta_{\text{IP, OP}}|}$ denotes the rotation directions of the predicted angles $\Delta \theta_{\text{IP}}$ and $\Delta \theta_{\text{OP}}$. With this, the CNN is forced not to give rotation predictions that point into the opposite direction as required. Note, that D_T and D_P are only used for training. When the CNN is used for prediction, these calculations are not performed.

2.4 Phantom Experiments

For validation, a phantom study is performed where several automated US scans at two different phantoms are executed. For each scan, the probe is positioned by hand at a start position on the phantom and the following scanning procedure is executed as shown in Figure 5. First, the contact force of the probe is adjusted to be in a range between 3 and 5 N by adapting the probe pose in the ^{tcp}z -direction (see \bigcirc 1) in Figure 5). Afterwards, an US volume is acquired and the rotation angles to align the probe are estimated by the CNN. If the absolute values of the predicted angles are greater than 3°, the probe is rotated appropriately (see (2) in Figure 5). Otherwise, the probe orientation remains constant. This threshold is chosen due to the step size of 3° in the training data acquisition. In the third step, the next path point is approached by moving the probe 5 mm into the ^{tcp}x - direction (see \bigcirc in Figure 5). In total, two validation trajectories on the torso phantom and one on

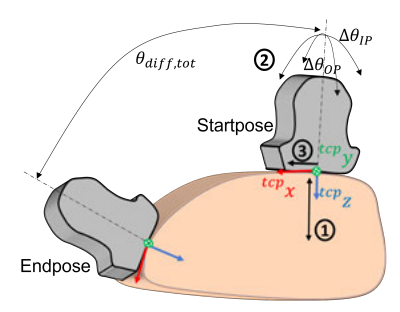


Fig. 5: Procedure of validation scans: The probe ^{tcp}z -axis is automatically aligned with the surface normal while scanning a curved tissue. $\theta_{diff,tot}$ is the difference between the surface normal at the start and the end position.

the transparent leg phantom are chosen (see black tape in Figure 1). At each location, five scans are performed. To evaluate the accuracy of the orientation alignment, the surface normals of the corresponding paths are determined by a laserscan done with a $Artec\ Leo$ laserscanner. The path is then divided equally into 24 areas for the scans on the torso phantom (rib and abdomen) and in 16 areas for the scan on the leg phantom. The mean surface normals of these areas are used to calculate the absolute angle error to the probe's ^{tcp}z -axis for each position of the trajectory.

3 Results

For evaluation, the absolute angle errors measured between the mean surface normals and the ^{tcp}z -axis of the US probe are investigated. The measured in-plane and out-of-plane angle errors are summed and considered jointly. In Figure 6, the absolute angle errors of all five iterations of the three validation scans are visualized. The mean absolute angle errors over all experiments is $5.0^{\circ} \pm 2.8^{\circ}$ and in 95 % of the probe positions the angle error is $\leq 9.7^{\circ}$. However, the results indicate that the accuracy on the leg phantom is higher than on the torso phantom. In the leg experiments, the mean angle error is $3.8^{\circ} \pm 2.9^{\circ}$ while the error on the rib and abdomen is

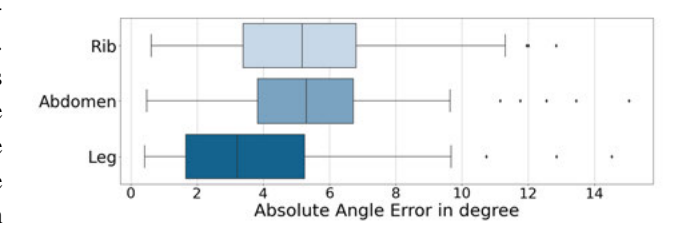


Fig. 6: Absolute angle error results for rib, abdomen and leg experiments. In each location five iterations are performed. The sum of the in-plane and out-of-plane errors are visualized.

 $5.3^{\circ} \pm 2.7^{\circ}$ and $5.5^{\circ} \pm 2.6^{\circ}$, respectively. Altogether, during the scans the probe had to rotate for 61.8° , 30.7° and 74.2° in the rib, abdomen and leg experiments, respectively. The robot was able to hold the probe in full surface contact the whole time during all experiments. Outliers, meaning probe positions where the angle error is quite high, could always be compensated in the following probe position.

4 Discussion

The goal of this work is to automatically align the central ^{tcp}z axis of an US probe approximately normal to the surface of the scanned tissue and to ensure high quality US volumes. Thus, curved surfaces can be scanned automatically without knowing the surface geometry. The results show that trajectories at unknown curved surfaces can be driven automatically by an US robot. The proposed method is applicable even in areas where orientation adaptions of more than 70° are required. The overall mean angle error is $5.0^{\circ} \pm 2.8^{\circ}$. Since the probe orientation is only adapted if the estimated rotation is $\geq 3^{\circ}$, this can be considered as high accuracy. This threshold is set due to the fact that the smallest rotation angle in the training data is 3° and thus, correct estimations by the CNN for smaller angles are not expectable. In addition, although the method is validated by measuring the error between the surface normal and the probe orientation, the CNN is not trained to align the probe to the surface normal. When acquiring the training data, the ground truth for the optimal probe orientation was set by hand. Thus, the CNN estimates the required rotation to reach US volumes without any non-contact artifacts as can be seen in Figure 3. This can be achieved even if the US probe is not optimally aligned to the surface normal, thus, errors are expected when comparing the probe orientation and the surface normal. This effect even increases at higher pressure forces which makes it necessary to use force information for an accurate rotation angle estimation. Compared to results from [6] the performance of the methods are comparable. Though in contrast to [6], our approach is based on 3D US images so that it is not necessary to perform a fan motion pattern for probe alignment. Another benefit of the proposed method is the invariance to the anatomical area of interest. The results show that the CNN is generalized for the rib, abdomen and leg areas where the anatomy is highly different. This was achieved by using the transducer area of the US volumes instead of the whole US volume. These anatomical areas of interest were, however, part of the training data set, so the method was not tested on completely unknown areas of interest.

5 Conclusion and Outlook

Robot guided US is becoming more interesting for a variety of clinical applications. Automatic US probe alignment, however, remain a challenging task. In this paper, a novel one step approach for US probe alignment based on 3D US images and force information is proposed. A CNN is trained that estimates the required rotation angles to align the US probe approximately normal to the surface. The method is validated in a phantom study where a high mean accuracy of $5.0^{\circ} \pm 2.8^{\circ}$ could be achieved. However, there is still potential for improvement. The training data set should be extended with samples at rotation angles less than 3° as well as data from further areas of interest to extend the data variability. In further studies the method will be tested on unknown phantom structures as well as on *in-vivo* data to investigate the usability of this approach.

Author Statement

Research funding: This study was founded by Deutsche Forschungsgemeinschaft (ER 817/1-2 and ER 817/4-1). Conflict of interest: Authors state no conflict of interest. Informed consent: Informed consent has been obtained from all individuals included in this study. Ethical approval: No experiments related to human use were conducted.

References

- [1] von Haxthausen F, Böttger S, Wulff D, Hagenah J, García-Vázques V, Ipsen S. Medical Robotics for Ultrasound Imaging: Current Systems and Future Trends. Current Robotics Reports 2021;2:55-71.
- [2] Burcher M R, Noble J A, Han L, Gooding M. A system for simultaneously measuring contact force, ultrasound, and position information for use in force-based correction of freehand scanning. IEEE transactions on ultrasonics, ferroelectrics, and frequency control 2005;52(8):1330-42.
- [3] Scorza A, Conforto S, D'Anna C, Sciuto S A. A Comparative Study on the Influence of Probe Placement on Quality Assurance Measurements in B-mode Ultrasound by Means of Ultrasound Phantoms. The open biomedical engineering journal 2015;9:164-178.
- [4] Ihnatsenka B, Boezaar A P. Ultrasound: Basic understanding and learning the language. International journal of shoulder surgery 2010;4(3):55-62.
- [5] Chatelain P, Krupa A, Navab N. Confidence-Driven Control of an Ultrasound Probe. IEEE Transactions on Robotics 2017;33(6):1410-24.
- [6] Jiang Z, Grimm M, Zhou M, Esteban J, Simson W, Zahnd G, Navab N. Automatic Normal Positioning of Robotic Ultrasound Probe Based Only on Confidence Map Optimization and Force Measurement. IEEE Robotics and Automation Letters 2020;5(2):1342-49